

FLEROV LABORATORY OF NUCLEAR REACTIONS

In 2008, the FLNR scientific program on heavy-ion physics included experiments on the synthesis and study of properties of heavy and exotic nuclei using ion beams of stable and radioactive isotopes, studies of nuclear reaction mechanisms, heavy-ion interaction with matter, applied research and development of acceleration technology. These lines of research were represented in 3 laboratory topics and 1 all-institute project:

- Synthesis of new nuclei and study of the nuclear properties and heavy-ion reaction mechanisms (11 sub-topics);
- Radiation effects and modification of materials, radioanalytical and radioisotopic investigations at the FLNR accelerators (5 sub-topics);
- Development of the FLNR cyclotron complex for producing intense beams of accelerated ions of stable and radioactive isotopes (2 sub-topics);
- Development and construction of an accelerator complex for producing radioactive ion beams (the DRIBs project).

In 2008, the operation time of the U400 and U400M FLNR cyclotrons was nearly 9000 h which is in accordance with the plan.

Study of the Complete Fusion Reaction $^{226}\text{Ra} + ^{48}\text{Ca}$

Further investigations in the domain of superheavy elements call for using beams of ions that are heavier than ^{48}Ca , as the heaviest isotope that can be used in such experiments as a target is ^{249}Cf . Fusion of ^{249}Cf with ^{48}Ca ions leads to the nuclei of element 118 synthesized in 2005.

However, with a heavier projectile the production cross section of the resulting nuclei could considerably decrease. In order to determine this possible reduction, we started the experiments on measuring the cross sections of the complete fusion reactions $^{226}\text{Ra} + ^{48}\text{Ca}$ and $^{226}\text{Ra} + ^{50}\text{Ti}$ with evaporation of 3–5 neutrons. Comparing the cross sections of the complete fusion reactions with ions of ^{48}Ca and ^{50}Ti one can estimate more accurately the cross sections of the complete fusion of the nuclei of ^{243}Am , ^{249}Bk , ^{249}Cf with ^{50}Ti ions and

thus clear the prospects of the synthesis of new elements 117, 119 and 120.

The first series of the experiments aimed at the study of the complete fusion of ^{226}Ra and ^{48}Ca was accomplished at the gas-filled separator in June 2008. The target of ^{226}Ra with the thickness of 0.23 mg/cm^2 was irradiated with ions of ^{48}Ca accelerated at the U400 cyclotron. The dose of the ^{48}Ca nuclei on the target was $3.0 \cdot 10^{18}$ at the energy of 233 MeV and $2.9 \cdot 10^{18}$ at 229 MeV. According to the calculations these energies correspond to the maximum yield of products of the complete fusion reaction $^{226}\text{Ra} + ^{48}\text{Ca}$ with evaporation of four and three neutrons, respectively resulting in the formation of the isotopes ^{270}Hs and ^{271}Hs .

Earlier these isotopes were observed in the reaction $^{248}\text{Cm} + ^{26}\text{Mg}$ that leads to the same compound nucleus ^{274}Hs . In those experiments the energy of the α -particles of ^{270}Hs was measured, $E_\alpha = 8.88 \pm 0.05 \text{ MeV}$. The half-life could not be determined, as the time of the formation of the nuclei was not registered. For the daughter nucleus ^{266}Sg spontaneous fission with a half-life of $0.36_{-0.10}^{+0.25} \text{ s}$ was observed. The cross section of this reaction makes about 3 pb.

The decay chains of four nuclei of ^{270}Hs observed in our experiments are given in Fig. 1. The measured α -particle energy is $9.03 \pm 0.09 \text{ MeV}$ and the half-life of this nucleus is $9.7_{-3.1}^{+9.0} \text{ s}$. For the spontaneously fissioning isotope ^{266}Sg the half-life was measured to be $0.21_{-0.07}^{+0.20} \text{ s}$.

The cross section of the reaction $^{226}\text{Ra}(^{48}\text{Ca}, 4n)^{270}\text{Hs}$ at the ^{48}Ca energy of 233 MeV is $9.0_{-4.9}^{+11.5} \text{ pb}$. At the energy of 229 MeV the nuclei of element 108 were not observed. The upper cross section limits are $\sigma_{3n} \leq 9.8 \text{ pb}$ and $\sigma_{4n} \leq 5.5 \text{ pb}$. The experiments are to be continued in December 2008.

The experimental results were published in [1, 2].

Separator VASSILISSA

During February–March 2008, we performed our 4th one-month long campaign with the recoil separator VASSILISSA and the experimental setup GABRIELA,

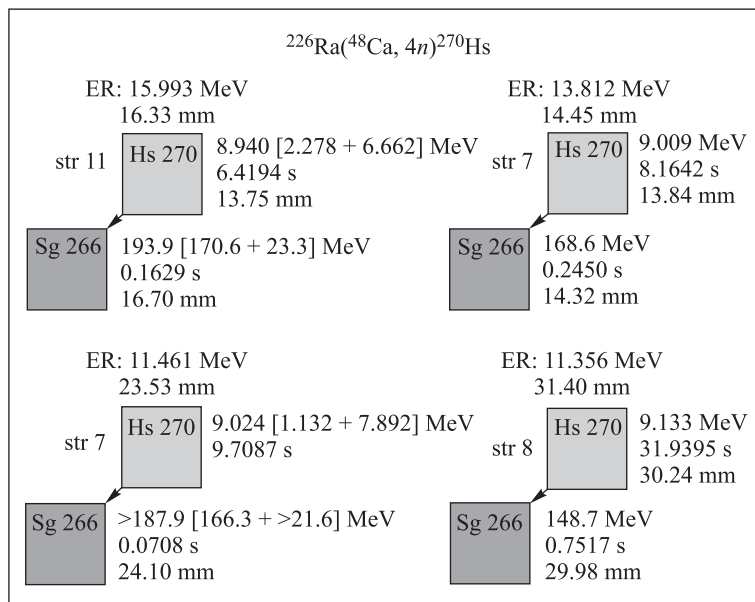


Fig. 1. Decay chains of the nuclei ^{270}Hs and ^{266}Sg at the ^{48}Ca energy of 233 MeV

(α -, β -, γ -spectroscopy). For the experiment with asymmetric target-projectile combinations the thickness of emissive foils used in TOF measurements was reduced to $\sim 15 \mu\text{g}/\text{cm}^2$ as compared with previous experiments. Tests were performed with the use of the reaction $^{22}\text{Ne} + ^{197}\text{Au}$. The transmission efficiency made about 6%. During the experiment the isotopes of $^{255,256}\text{No}$ were produced with the beam of ^{22}Ne ($\sim 2.0 \text{ p}\mu\text{A}$) impinging on the rotating ^{238}U target and spectroscopy data were collected. With the use of the ^{40}Ar beam and ^{208}Pb , ^{181}Ta , ^{178}Hf targets, we studied the decay properties of $^{245,246}\text{Fm}$ and obtained complementary statistics for the decay of ^{217}Pa and ^{214}Th . The analysis of these data is still in progress.

In October 2008, the spontaneous fission of $^{244,246}\text{Fm}$ isotopes produced in the complete fusion reaction $^{40}\text{Ar} + ^{208}\text{Pb}$ was investigated. For this purpose a big neutron detector with 62 ^3He counters, surrounding the focal plane semiconductor detector assembly, has been developed and installed. This detector allows one to measure neutron multiplicities accompanying the fission process. The experiment lasted 10 days and brought new information on the process of spontaneous fission in heavy isotopes.

The modernization of the VASSILISSA separator was started in 2008. It is planned to replace the central part of the separator, consisting of 3 electrostatic deflectors, by a combination of two electrostatic deflectors and two dipole magnets, thus creating a velocity filter instead of an energy filter. The modernized VASSILISSA will have an optical scheme QQQ-E-D-D-E-QQQ (where Q stands for Quadrupole lens, E for Electrostatic dipole, D for Dipole magnet) and locate at the beam channel N3 of the U400 cyclotron. The manufacturing of the new dipole magnets was started and two power supplies for these magnets were purchased.

The analysis of the data taken during the further 3 campaigns goes on. The isomeric state of ^{209}Ra was observed in the reaction $^{174}\text{Yb}(^{40}\text{Ar}, 5n)$ and it was found that this state decays to the ground state of ^{209}Ra via a cascade of 238 keV (M2) and 644 keV transitions. The half-life of the isomer was found to be 117(5) μs and assigned to $I^\pi = 13/2^+$ shell-model state according to systematics. The isomeric state was also observed in ^{255}Lr produced in the reaction $^{209}\text{Bi}(^{48}\text{Ca}, 2n)$. It has half-life $T_{1/2} = 1.52(12) \mu\text{s}$ and the excitation energy $E^x > 720 \text{ keV}$. One can assume that this isomer has a 3 quasi-particle configuration. Some preliminary results concerning the α -decay of ^{217}Pa have also been obtained.

The experimental results were published in [3–5].

Chemistry of Elements 112 and 114

In April–June 2008, the joint experiment on the chemical study of the element 114 was performed with the radiochemical groups from PSI, Switzerland and LLNL, USA. Basing on the study of the behavior of isotopes $^{288}\text{114}$ and $^{287}\text{114}$ for the first time in 2007 we established that volatility of element 114 is closer to that of heavy noble gases than to its closest homolog lead. However, due to the relatively high spontaneous fission background we could not identify unambiguously the isotope $^{289}\text{114}$ having two longer-lived descendants $^{285}\text{112}$ ($T_{1/2} \sim 29 \text{ s}$, α) and ^{281}Ds ($T_{1/2} \sim 11.1 \text{ s}$, SF).

In the last experiment the possibilities of chemical and physical separation of the nuclear reaction products were combined. Rotating targets of $^{244}\text{PuO}_2$ ($0.4 \text{ mg} \cdot \text{cm}^{-2}$) deposited on a $1.5 \mu\text{m}$ Ti backing foil were irradiated with a beam dose of $9.7 \cdot 10^{18}$ of ^{48}Ca . The energy of the beam in the centre of the target was $238 \pm 4 \text{ MeV}$. The products of the nuclear reactions

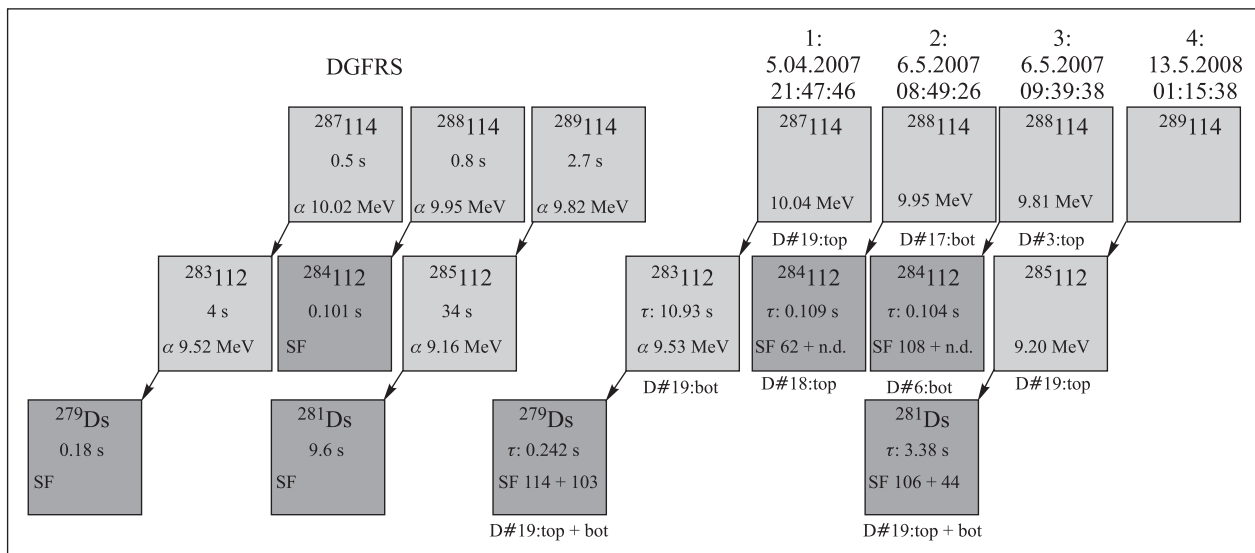


Fig. 2. The decay properties of $^{287-289}114$

$^{244}\text{Pu}(^{48}\text{Ca}, 3-4n)$ $^{288-289}114$ were studied. Chemical separation equipment was placed in the focal plane of Dubna Gas-Filled Recoil Separator (DGFRS). The recoiled atoms were thermalized in a recoil chamber through which a transporting gas was flowing at 2.1 l/min. The carrier gas transported the separated volatile reaction products to the thermochromatography device including the cryodetector COLD. A temperature gradient from 11 to -171°C was established along the COLD. The total efficiency of measurement appeared to be a factor 2–3 less as compared with the previous experiment due to the more thin target (in the previous experiment we used the target of the thickness of $1.4\text{ mg}\cdot\text{cm}^{-2}$) and efficiency of the separator (35%).

During the experiment one decay chain was observed that can be unambiguously attributed to the decay of $^{285}112$ and its daughter ^{281}Ds (Fig.2, decay chain 4), which are the descendants of $^{289}114$. This decay chain was observed at the deposition temperature of -93°C , i.e., close to the deposition maximum expected for $^{289}114$. Additionally, only two coincident fission events were observed: at the deposition temperature -8°C (the fragment energies 131 and 50 MeV) and at the temperature -16°C (the fragment energies 88 and 101 MeV) which we assign to the decay of $^{284}112$ ($T_{1/2} = 0.1\text{ s}$, SF). Since an isotope with such a short half-life could not reach the detection chamber at the transportation time of 1.2 s, we assume that it is a daughter product of the isotope $^{288}114$ ($T_{1/2} = 0.8\text{ s}$), which decayed in the transporting capillary (near the detection chamber) emitting undetected α -particle and descended to $^{284}112$. Hence, the detection of the daughter isotope $^{284}112$ also indicates high volatility of the element 114. Chemical deposition of $^{284}112$ observed in COLD is in a full agreement with the results of previous experiments dedicated to the element 112. However, an unambiguous identification of $^{284}112$ was impossible.

Basing on the results of 2007 and 2008 year experiments we calculated the adsorption enthalpy of the element 114 on the gold surface $-\Delta H_{\text{ads}}^{\text{Au}}(\text{E}114) = 35_{-3}^{+6}\text{ kJ/mol}$. Theoretical calculations predict the value $-\Delta H_{\text{ads}}^{\text{Au}}(\text{E}114) = 92\text{ kJ/mol}$ for the formation of metallic bonds between the element 114 and surfaces of transition metals. According to these calculations the deposition temperature of the element 114 on gold makes about 150°C . Some other approaches give $-\Delta H_{\text{ads}}^{\text{Au}}(\text{E}114) = 42 \pm 5\text{ kJ/mol}$. Comparing theoretical predictions with experimental result we conclude that chemical properties of the element 114 are close to those of noble gases. In the atomic state it forms a weak adsorption bond with a gold surface. The experimental result points out to a substantially increased stability of the atomic state of the element 114 due to the strong relativistic shell closure in the valence electronic structure.

Nuclear Fission

In 2007, the measurements of mass and energy distributions of fission and quasifission fragments in coincidence with neutrons and gamma-rays in the reaction $^{36}\text{S} + ^{238}\text{U}$ were performed using time-of-flight position-sensitive CORSET spectrometer and DEMON spectrometer [6]. During 2008 the main attention was paid to processing and analysis of the experimental data, obtained in the reaction $^{36}\text{S} + ^{238}\text{U} \rightarrow ^{274}\text{Hs}$. The experiment was carried out at the Flerov Laboratory of Nuclear Reactions in a wide collaboration: the scientific centers of France, Italy, Belgium, Brasilia and SAR put at common disposal the DEMON setup, gamma-detectors, light charged particles detectors and a part of the electronic setup. The measurements of mass and energy distributions allowed us to get the information on the compound nucleus fission as well as on the quasifission process.

The reaction $^{36}\text{S} + ^{238}\text{U} \rightarrow ^{274}\text{Hs}$ was chosen to investigate the role of mass asymmetry of the entrance channel in the dynamics of the formation of superheavy compound system. Both this reaction and the reaction $^{26}\text{Mg} + ^{248}\text{Cm}$ studied in the previous experiments lead to the formation of the same compound system. The comparative analysis of these reactions shows that for the reaction with ^{26}Mg ions the mass distributions have a near Gaussian form at energies below and above the Coulomb barrier, while in the reaction with ^{36}S ions the mass distribution dramatically varies from the asymmetric form at energies below the Coulomb barrier to the symmetric one above the barrier. One of possible reasons is the influence of mass asymmetry of entrance channel, which leads to the increase of the quasifission process yield for more symmetric reaction $^{36}\text{S} + ^{238}\text{U}$. For both reactions the mass distribution of quasifission fragments bunches around the closed proton ($Z = 28$) and neutron ($N = 50, 126$) shells mainly (see Fig. 3).

In 2008, the analysis of the data obtained in the reactions $^{44}\text{Ca} + ^{206}\text{Pb}$ and $^{64}\text{Ni} + ^{186}\text{W}$, leading to the compound system ^{250}No , was done and published. For both systems the quasifission process was observed. In the reaction with ^{64}Ni ions the quasifission is a dominant process, while for ^{44}Ca the main channel is a

fusion–fission of compound nucleus ^{250}No . It was found that the closed shells with $Z = 28, 50$ and $N = 50, 82$ influence strongly the formation of binary reaction products both for fusion–fission of the compound nucleus and quasifission processes. The symmetric and asymmetric fission modes manifest themselves in the mass distribution of the fission fragments of ^{250}No , and the asymmetric one is connected with the neutron closed shell with $N = 82$ [7].

In 2008, the interaction of two spherical nuclei $^{48}\text{Ca} + ^{208}\text{Pb} \rightarrow ^{256}\text{No}$ in a wide energy region of ^{48}Ca (206–242 MeV) was studied and the results were published. Mass–energy distributions of binary reaction products were obtained as well as cross sections of capture and fusion–fission processes. It was found that the characteristics of symmetric fragments in the mass range 100–156 a.e.m. are close to those of the fusion–fission process in the frame of liquid drop model, while quasifission process is suppressed strongly. The structural peculiarities caused by shell effects were found in the mass distributions. The high-energy «super-short» fission mode with a mass of the heavy fragment 130–135 a.m.u. was found. The contribution of this mode is about 2.5% at the energy of 211 MeV and it decreases to 0.3% at the energy of 234 MeV [8].

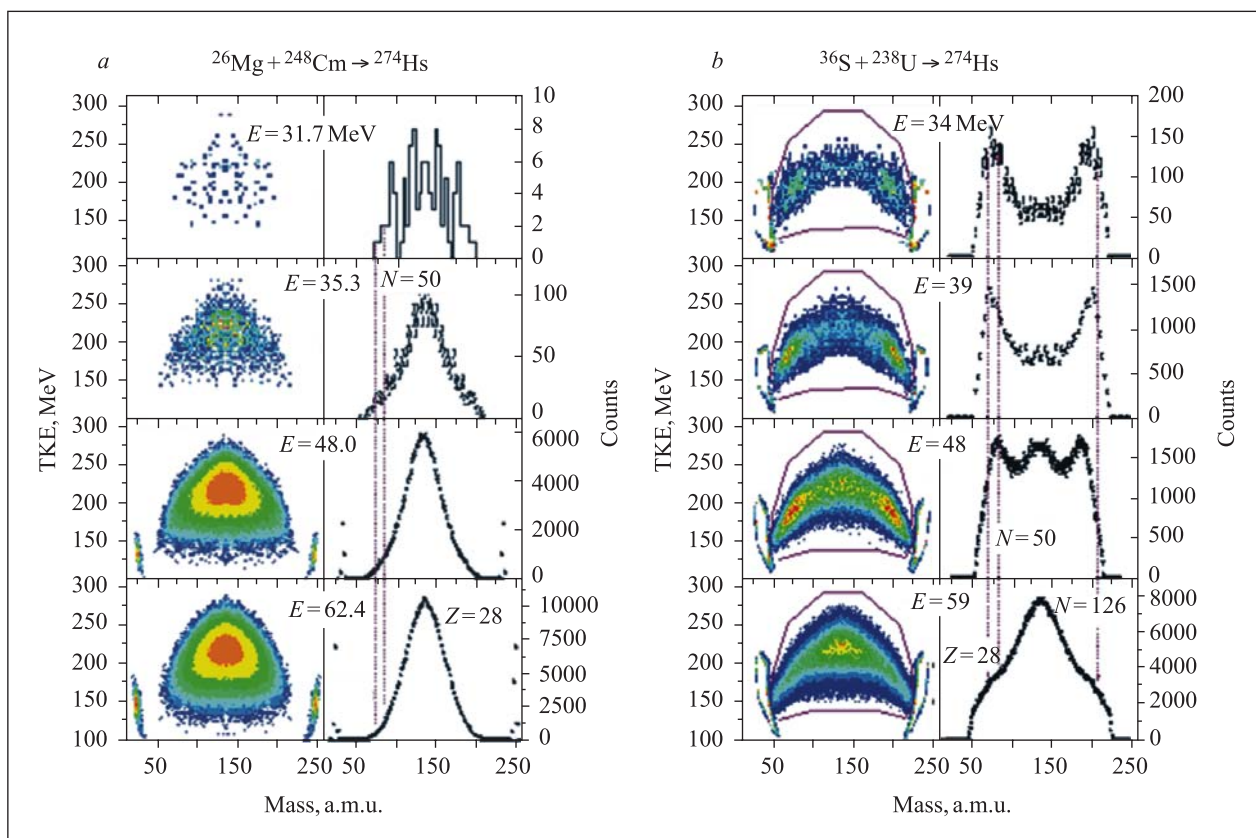


Fig. 3. The mass–energy distributions of binary products for the reactions $^{26}\text{Mg} + ^{248}\text{Cm}$ (a) and $^{36}\text{S} + ^{238}\text{U}$ (b), leading to the formation of the same compound system ^{274}Hs at different excitation energies near the Coulomb barrier. The two-dimensional matrices of mass–total kinetic energy for binary products are shown in a; b shows the mass distributions of fission-like events inside the outlined contour on the M–TKE matrices

In 2008, the analysis of the experimental data on the study of the characteristics of fission of the compound nucleus ^{274}Hs was accomplished and published. It was found that mass distribution of fission fragments of compound nucleus ^{274}Hs formed in the reaction $^{26}\text{Mg} + ^{248}\text{Cm}$, has a modal structure. Also we found that for the fragment with $\text{TKE} > 220$ MeV the mass distribution is very narrow, while for the fragments with $\text{TKE} < 220$ MeV the mass distribution has a Gaussian shape. The dispersion of the distribution is in a good agreement with that obtained within the liquid drop model. The narrow mass distribution of fission fragments with high TKE is a result of the fission of ^{274}Hs in two identical fragments. In this case both fragments have a number of neutrons close to $N = 82$ (the closed neutron shell). The total kinetic energy distribution also consists of two parts concentrated around 198 and 227 MeV. The strong increase of the high-energy symmetric mode is a general tendency in the fission of superheavy nuclei when the number of neutrons is close to 82 for both fragments [9].

In the frame of the collaboration between FLNR JINR and University of Jyväskylä the experiment on the study of the dynamics of the $^{64}\text{Ni} + ^{238}\text{U}$ reaction was carried out in October 2008. The energy of ^{64}Ni ions was varied from 320 to 390 MeV (below and above the Coulomb barrier). The mass–energy distributions of binary reaction products and the energy of emitted α -particles were measured with the use of the double-arm time-of-flight position-sensitive spectrometer CORSET and $\Delta E \times E$ detectors of light charge particles (INFN, Italy) installed in the reaction chamber HENDES (Finland). At the present time the experimental data are under analysis.

The fusion cross section measurements in the reaction $^{48}\text{Ca} + ^{238}\text{U}$ at the Coulomb barrier energies were

performed in November–December 2008. The main task of this experiment was to obtain the complete fusion cross section for the $^{48}\text{Ca} + ^{238}\text{U}$ reaction. The mass and energy distributions for fission-like fragments mainly produced in the exit reaction channel of the reaction at the Coulomb barrier energies were measured. Existing data concerning the capture and fission cross sections for this reaction show a strong disagreement. This experiment was performed at the TANDEM-ALPI accelerator of the LNL (INFN, Legnaro, Italy) with the use of spectrometer CORSET.

Exotic Decay Modes

An essential step was done this year in development of the data processing procedure aimed at revealing of fine structure (FS) in mass vs. total kinetic energy (M-TKE) distributions of nuclear reaction products. For the fusion–fission reactions the analysis of the FS found previously let us come to conclusion that the FS likely depicts in the elongation-mass asymmetry space a scission line caused by a specific fission mode. The question concerning a reliability of the FS detection was still open.

An original approach based on the morphological analysis of the images is proposed. The method let one to estimate numerically a reliability of the FS detection and improve the filter used for this purpose. For instance, the FS obtained in the frame of the heuristics approach is shown in Fig. 4, *a*. Information concerning the symmetry of the distribution was taken into account a priori in this case. The initial M-TKE distribution of the fragments was measured for the reaction $^{238}\text{U} + p$ (60 MeV). Results of corresponding morphological analysis are presented in Fig. 4, *b*. Any additional information was not attracted. Good agreement

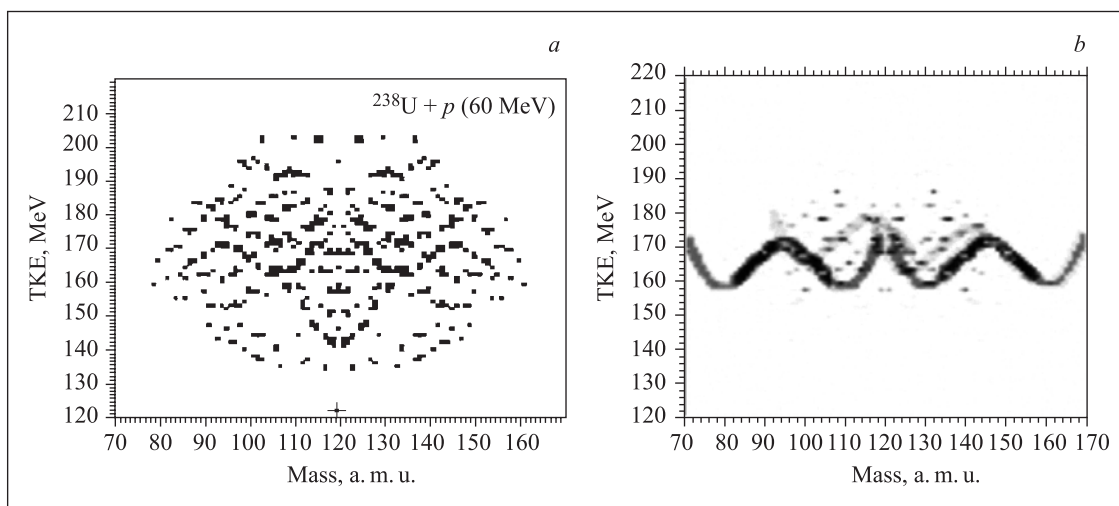


Fig. 4. Fine structure of the M-TKE distribution revealed in the frame of the heuristics approach (*a*). The same initial data are processed using morphological methods of image analysis (*b*). The probability of random appearance of the FS is proved to be less than 10^{-3}

between images is seen. In addition, the quantitative estimation of the FS detection reliability was obtained as well. It is proved the probability of random appearance of the structure in question to be less than 10^{-3} .

The experimental results were published in [10, 11].

Fragment Separator ACCULINNA

Complete fusion and breakup reactions initiated by ${}^6\text{He}$ halo nuclei were investigated in the interaction with medium mass target ${}^{166}\text{Er}$ at a ${}^6\text{He}$ beam energy $E_{\text{lab}} = 55 - 64$ MeV. The ${}^6\text{Li} + {}^{165}\text{Ho}$ and ${}^6\text{Li} + {}^{166}\text{Er}$ reactions were studied at a projectile energy 58 MeV. The layout of the setup used in these experiments is shown in Fig. 5. The experiments were performed using the DRIBs facility and a detector system based on six HP Ge detectors with BGO shells for the subtraction of Compton scattering effect, a charged particle telescope and an array of neutron detectors consisting of eight units of the time-of-flight spectrometer DEMON. The detection efficiencies for a single γ -ray with energy of $E_\gamma > 80$ keV and a γ_1 - γ_2 coincidence event were within the limits of 0.06–0.015 and $3 \cdot 10^{-3} - 2 \cdot 10^{-4}$, respectively. The charged particle telescope was composed of three annular shape Si detectors. Having a thickness of 2.3 mm of Si this telescope detected charged particles (p , d , t , ${}^3\text{He}$, as well as the beam nuclei, ${}^6\text{H}$ and/or ${}^6\text{Li}$, undergoing elastic and inelastic scattering on the target nuclei). The telescope detected the charged particles emitted from the target in the angular range $15-40^\circ$. The Demon modules detected with a 1% efficiency fast (3–10 MeV) neutrons emitted to the forward direction from the target within a $\pm 15^\circ$ cone. Data acquisition was triggered by the signals showing the detection of any γ_1 - γ_2 coincidence event.

Population probabilities were measured for the levels of the ground-state rotational band and for band-8 in ${}^{166}\text{Yb}$. The critical values of the orbital momentum, l_{crit} , and diffuseness parameter D_l characterizing the width of the orbital momentum region where the transmission coefficients T_l change to zero from the unit value inherent to the small l partial waves allowed for CF. Parameters l_{crit} and D_l responsible for the ${}^{166}\text{Yb}$ formation were deduced from the data analysis done with the use of code EMPIRE. Results obtained for the CF reactions ${}^{166}\text{Er}({}^6\text{He}, 6n){}^{166}\text{Yb}$ and ${}^{165}\text{Ho}({}^6\text{Li}, 5n){}^{166}\text{Yb}$ are shown in Fig. 6. Numerical results are listed in Table. For the case of the ${}^{166}\text{Er}({}^6\text{He}, 6n){}^{166}\text{Yb}$ reaction roughly the same critical orbital momentum $l_{\text{crit}} = 19.3$ and diffuseness $D_l = 1.5$ were obtained from the EMPIRE fits done for the data of 64 and 55 MeV ${}^6\text{He}$. In the case of the ${}^{165}\text{Ho}({}^6\text{Li}, 5n){}^{166}\text{Yb}$ reaction ($E_{\text{lab}} = 58$ MeV) the critical orbital momentum for fusion becomes ~ 18.6 . The complete fusion cross sections that follow from these values of the critical orbital momentum make about 731 and 737 mb for the ${}^6\text{He}$ and ${}^6\text{Li}$ induced reactions, respectively.

We define the suppression factor to the CF cross section as the ratio between the value calculated with code EMPIRE (see column EMPIRE default) and the cross section deduced from the obtained l_{crit} and D_l values (see column «Fit to experiment» in Table). The cross section given by the EMPIRE default is the result obtained in the framework of the single barrier penetration model. As one can see from data given in Table the suppression factor obtained for the ${}^{166}\text{Er} + {}^6\text{He}$ reaction is larger than that obtained for the ${}^{165}\text{Ho} + {}^6\text{Li}$ reaction. We consider this difference meaningful and showing that there is a difference between the ${}^6\text{He}$ and

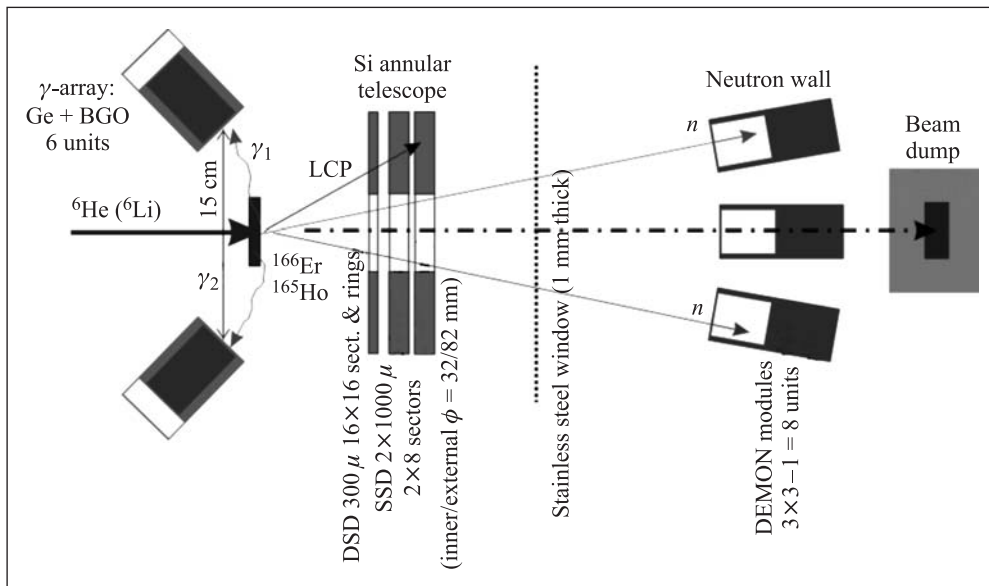


Fig. 5. Scheme of experiments for the complete and incomplete fusion study

Complete fusion cross section σ_{fusion} , neutron evaporation cross section σ_{5n} (σ_{6n}), average values of critical angular momentum l_{crit} and diffuseness parameter D_l obtained experimentally and with the EMPIRE default. Suppression factors to the CF reactions are given in column 4

Projectile, energy, MeV	$\sigma_{\text{fusion}}/l_{\text{crit}}$, mb/ \hbar		CF suppression factor	σ_{xn}/D_l , mb/ \hbar	
	EMPIRE default	Fit to experiment		EMPIRE default	Fit to experiment
${}^6\text{He}$, 64	2490 / 39.0	731 / 19.3	3.41	881 / 1.5	254 / 1.5
${}^6\text{Li}$, 58	1770 / 32.5	737 / 18.6	2.40	656 / 0.2	244 / 0.4

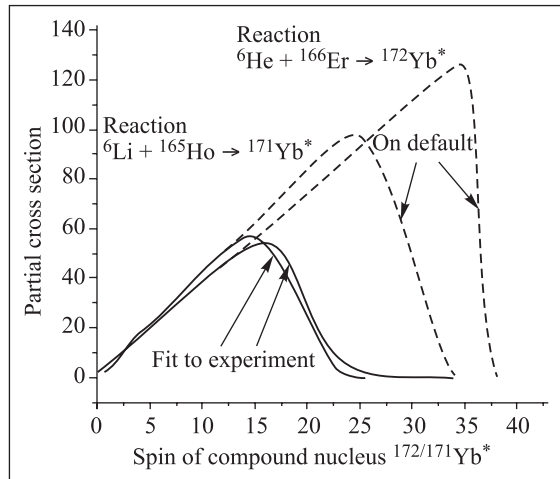


Fig. 6. Cross section dependence on the orbital momentum values of the partial waves that contribute in the CF reaction. Solid lines show the distributions obtained from the fit to the measured populations of different spin levels of the rotational bands in ${}^{166}\text{Yb}$. Dashed lines show the same distributions calculated with the use of the EMPIRE default setting

${}^6\text{Li}$ projectiles from the point of view of the fusion probability. The broad gaps are obtained in the high angular momentum regions where complete fusion does not take place (see Fig. 6). A reasonable assumption is that in these regions incomplete fusion and/or breakup become the main reaction channels.

The experimental results were published in [12–16].

Reactions Induced by Stable and Radioactive Ion Beams of Light Elements

During 2008, at the accelerator complex DRIBs, the reaction channels ${}^{206}\text{Pb}({}^6\text{He}, 2n){}^{210}\text{Po}$ and ${}^{208}\text{Pb}({}^4\text{He}, 2n){}^{210}\text{Po}$, leading to the formation of one and the same compound nucleus ${}^{212}\text{Po}$, were studied. For these measurements a special technique for working with secondary radioactive nuclei was created and tested.

As a result, a monochromatized beam of ${}^6\text{He}$ ions with high intensity (up to 10^8 pps) was used. Two different methods were developed for decreasing the beam energy (even to energies below the Coulomb barrier) without significant deteriorating the intensity of the beams of ${}^6\text{He}$ and ${}^6\text{Li}$:

— a method including the magnetic spectrometer MSP-144 as a monochromatizer;

— a method in which the internal gauge of the U400 accelerator was used.

A setup for measuring induced α -activity consisting of 16 channels has also been created.

The stacked foil activation technique was used for the production and measuring the yields of reaction products. In the reaction ${}^{206}\text{Pb}({}^6\text{He}, 2n){}^{210}\text{Po}$ with energy resolution not worse than 0.8 MeV, a significant enhancement of the fusion cross section was observed in the sub-Coulomb-barrier region compared to the cross section for the ${}^{208}\text{Pb}({}^4\text{He}, 2n){}^{210}\text{Po}$ reaction. This fact gives evidence of the influence of weakly bound neutrons in ${}^6\text{He}$ on the fusion mechanism.

New data on the complete fusion of ${}^6\text{Li}$ with Pt and Bi were obtained together with new information on the breakup of the loosely bound ${}^6\text{He}$ and ${}^6\text{Li}$ nuclei followed by fusion of the produced fragments with the target nucleus. The obtained results show that enhancement of the cross section for the transfer of clusters from the weakly bound nuclei takes place ($2n$ — in the case of ${}^6\text{He}$, and d — in the case of ${}^6\text{Li}$).

The main results of the experiments performed in 2008 can be found in [17–20].

Theoretical and Computational Physics

«Cold» and «hot» synthesis, fusion of fission fragments, transfer reactions, and reactions with radioactive ion beams leading to the formation of new superheavy (SH) elements and isotopes are analyzed along with their abilities and limitations [21]. It is shown that if the possibility of increasing the beam intensity and the detection efficiency (by a total of one order of magnitude) is found, then several isotopes of new elements with $Z = 120–124$ could be synthesized in fusion reactions of titanium, chromium, and iron beams with actinide targets. The use of light- and medium-mass neutron-rich radioactive beams may help us to fill the gap between the SH nuclei produced in the hot fusion reactions and the mainland. In these reactions, we may really approach the «island of stability». Such a possibility is also provided by the multi-nucleon transfer processes in low-energy damped collisions of heavy actinide nuclei. It is found that the production of SH elements in fusion reactions with accelerated fission fragments looks less encouraging.

A new way is found to discover and examine unknown neutron-rich heavy nuclei at the «north-east» part of the nuclear map [22, 23]. This «blank spot» of the nuclear map can be reached neither in fusion-fission reactions nor in fragmentation processes widely used nowadays for the production of new nuclei. The present limits of the upper part of the nuclear map are very close to stability, while the unexplored area of heavy neutron-rich nuclides along the neutron closed shell $N = 126$ (to the east of the stability line) is extremely important for nuclear astrophysics investigations and, in particular, for the understanding of the r -process of astrophysical nucleogenesis. A novel idea is proposed for the production of these nuclei via low-energy multi-nucleon transfer reactions. The estimated yields of neutron-rich nuclei are found to be rather high in such reactions and several tens of new nuclides can be produced, for example, in the near-barrier collision of ^{136}Xe with ^{208}Pb . This finding may spur new studies at heavy-ion facilities and should have significant impact on future experiments.

For the first time it was shown that the «barrier distribution» derived from quasi-elastic backscattering of heavy ions gives us, in fact, information about the «total reaction threshold distribution» and not about the «fusion barrier» [24]. This is not a terminology problem but an important finding, because experiments on the measurement of backward-angle quasi-elastic scattering for deriving the barrier distributions for heavy nuclear systems (which may be used for the production of superheavy elements) are planned to be performed in several laboratories.

The method of molecular states of valence neutrons and the time-dependent quantum low-dimensional model were applied to description of sub-barrier fusion of ^6He with ^{12}C [25]. The calculations confirm the predictions of our semiempirical model about a significant enhancement of the fusion cross section of neutron-rich weakly bound nuclei. This may be quite important for astrophysical primordial and supernova nucleosynthesis.

Contribution of the breakup channels of light weakly bound nuclei into the optical potential of their elastic scattering from heavy ions was calculated with the Feshbach projection operator technique [26]. The method proposed earlier was extended to avoid the previously used simplifications. The bound and continuum states of the projectile are described in the framework of microscopic cluster model and are used to construct the Feshbach projection operators. The generalized optical potential which takes into account explicitly the coupling with projectile breakup channels was derived. An applicability of the model was demonstrated for elastic scattering of the ^2H and ^6Li nuclei. The approach was also applied to the ^6He elastic scattering at intermediate energy using the realistic few-body wave functions of ^6He . It was found that the simplified two-cluster model overestimates the breakup contribution to the optical

potential and, consequently, underestimates the elastic cross section at large scattering angles.

A stochastic approach to fission dynamics based on three-dimensional Langevin equations was applied to calculation of the mass-energy and angular distributions of fission fragments [27]. The dependence of the mass-energy distribution parameters on the angular momentum and the anisotropy of the fission-fragment angular distribution on excitation energy have been studied. A temperature-dependent finite-range liquid drop model was used in a consistent way to calculate the functional of the Helmholtz free energy and level-density parameter. The modified one-body mechanism of nuclear dissipation was used to determine the dissipative forces in Langevin equations. The evaporation of light pre-scission particles was taken into account. Analysis of the anisotropy of the fission-fragment angular distribution performed with the saddle-point transition state model and scission-point transition state model indicates that it is necessary to take into account the dynamical aspects of the fission-fragment angular distribution formation.

The knowledge base on low energy nuclear physics, «Nuclear Reactions Video», allocated at the Web-site <http://nrv.jinr.ru/nrv>, was significantly extended and improved [28]. (i) Computational codes for a calculation of the survival probability and decay widths (neutron, proton, α -particle, γ -quanta, and fission) of excited nuclei were included into the knowledge base. Web-dialog for this model and Java-applets for drawing and downloading the obtained results have been written. (ii) Already existing in «Nuclear Models» section the optical model of elastic scattering was enriched by the possibility to calculate the elastic scattering cross section using the DDM3Y folding interaction. (iii) The digital databases on fusion reactions and yields of evaporation residues have been filled with several hundreds experimental cross sections. All the resources of the knowledge base are available on-line via the standard Web browsers using CGI technology and Java-applets.

The effects of shell correction energy for fusion process are investigated on the basis of the fluctuation-dissipation dynamics [29]. In the superheavy mass region, shell correction energy plays a very important role and enhances the fusion probability when the colliding partner has a strong shell structure. By analyzing the trajectory in the three-dimensional coordinate space with the Langevin equation, we reveal the mechanism of the enhancement of the fusion probability caused by «cold fusion valleys» and the temporary pocket which appears in fusion process.

Nanotechnologies and Radiation Modification of Materials

Electrical and optical properties of silicon nanocrystals (ncSi) embedded in SiO_2 layer (the single phase Si content in oxide ranged between 5 and 92 volume %) irradiated with high energy Bi and Kr ions in track non-

overlapping regime, have been studied in 2008. Ion-induced modifications of SiO₂-ncSi properties include a shift of the major ncSi-related photoluminescence peak and intensification of the high-photon energy peaks, that accompany the change in amount and type of the charge trapped on the nanocrystals.

Comparative studies of radiation damaging of GaN and ZnO layers grown by MOCVD and by electrodeposition from aqueous solutions after 130 MeV Xe⁺²³ irradiation to fluence $1.5 \cdot 10^{14} \text{ cm}^{-2}$ have been carried out. The luminescence and resonant Raman scattering analysis showed that nanostructured materials exhibit enhanced radiation hardness against high energy heavy-ion irradiation as compared to bulk layers.

Depth profiles of residual mechanical stress in Al₂O₃:Cr crystals irradiated with (1–3) MeV/amu Kr, Xe and Bi ions have been studied by using laser confocal scanning microscopy technique. As was found, the stress field generated by swift heavy-ion irradiation is composed of compressive stresses with maximal magnitude comparable with ultimate stress limit of ruby crystals. Experimental data are discussed in the framework of model, considering the Cr³⁺ atoms as individual piezosensors.

The blister structure evolution in Si irradiated with two-component ion beam (He + H/D) has been studied. The efficiency of blister production, associated with synergistic effect due to radiation damage induced by He ions and Si-H(D) bonds formation was demonstrated. Optimized regimes of two-layer Cu/Ni nanowires formation in electrolytic solution with Co and Ni anodes have been found.

Main results were published in [30–34].

Track Membranes and Modification of Polymers

The work on the development of track membranes with improved permeability and improved chemical stability in the framework of the agreement between Shubnikov Institute of Crystallography of RAS (customer) and Joint Institute for Nuclear Research (executor), entitled «Creation of Scientific Basics of Production Technology of Track Membranes from Polyethylene Terephthalate and Polyethylene Naphthalate. Upgrading Irradiation and Chemical Etching Setups», financed by the Federal program «Investigation and Development in Priority Directions of Development of Scientific and Technological Russian Complex for 2007–2012», was completed.

Development of production methods of asymmetric micro- and nanopores, using chemical treatment of heavy-ion irradiated polymers, is being continued. Methods allowing control over the pore profile are suggested. Electrochemical properties of asymmetric nanoporous membranes are investigated. It is shown that geometrical asymmetry leads to diode-like properties. Effect of electrical current rectification in asymmetric nanopores filled with an electrolyte is studied in

dependence on the electrolyte concentration, pore size and the degree of geometrical asymmetry. In collaboration with the Institute of Acoustics (Madrid, Spain), experiments on propagation of ultrasonic waves of different frequencies through track membranes that served as model porous media were carried out. It is shown that an ultrasonic wave going through a membrane is split into two components. One component is a wave propagating through membrane matrix, while the other one is propagating through the air filling the pores. Phase and magnitude of the second component can be measured and used for estimates of membrane properties such as porosity and pore diameter.

The structure and electrotransport properties of poly(ethylene terephthalate) and polycarbonate track membranes modified by thiophene and pyrrole plasma were studied. The influence of the degree of oxidation by iodine or UV-irradiation of the polymeric layer, formed by plasma, on the membrane characteristics was studied. It has been found that deposition of the polymeric layer on the surface of the track membranes with the help of polymerization of the thiophene or pyrrole vapors in plasma leads to formation of the composite membranes possessing an asymmetry of conductivity (rectification effect) in a potassium chloride solution. It is caused by the presence in the modified membranes of two layers with antipolar conductivity. It is shown that doping the polymer layer formed in plasma by iodine or the effect of UV-irradiation causes a change of the density of a positive charge on its macromolecules and thus leads to the change in the rectification effect degree.

A procedure of template synthesis of micro- and nanostructural materials (nanowires, nanotubes as well as nanomembranes with a selective layer) on a basis of copolymers from styrene, butylmethacrylate and 4-aminostyrene has been developed. Similar polymeric compositions can be used as matrices in nonlinear optics to create electronic and optical nanodevices. As template the poly(ethylene terephthalate) track membranes with effective pore diameter less than 1.0 μm were used. The laws of formation of these materials and their structural properties were investigated. To produce the polymeric nanomaterials, a flushing method was used. It is shown that varying the parameters of the process of deposition of copolymers on the track membranes surface provides a way for producing a big assortment of composite nanomembranes with a selective layer as well as nanowires and nanotubes with a wide spectrum of characteristics.

Creation of the Nanodimensional Structures by Ionic Implantation

Calculations of temperature effects in highly oriented pyrolytic graphite under irradiation by heavy ions were carried out in the frame of the thermal spike model. On the base of these calculations the effects

of creation (for ^{209}Bi with energy 710 MeV) or absence (for ^{86}Kr with energy 305 MeV) of hillocks in experiments which were made earlier were explained.

The model of a capture of ^{84}Kr ions as well as high energy firstly knocked Ga and As atoms in axial channeling regime was proposed for explanation of results obtained in experiments on the study of the cross section of GaAs single crystals irradiated with ^{84}Kr (394 MeV) ions.

The studies of SiC, Al_2O_3 single crystals and two slow magnetic amorphous alloy samples irradiated by electrons and swift heavy ions are being carried out.

Radioanalytical Research and Ultrapure Radioisotopes for Nuclear Medicine

Production of Radioisotopes:

1. The ultrapure (radionuclide-pure) radioactive isotopes in a condition without the carrier were produced: ^{88}Zr , ^{92m}Nb , ^{99}Mo (^{99m}Tc), ^{97}Ru , ^{109}Cd , ^{111}In , ^{175}Hf , ^{177}Ta , ^{178}W (^{178}Ta), ^{186}Re , ^{188}Re , ^{211}At , ^{237}U , $^{236,237}\text{Pu}$, etc.
2. The new methods of separation and concentration (selective nuclear reactions, recoil, radiochemical separation) of ^{99}Mo and ^{100}Mo , ^{237}U and ^{238}U with the factor of enrichment $10^4 - 10^5$ are developed.
3. 50 kBq of ^{236}Pu for radioecological and biomedical research is produced.
4. The reaction $^{118}\text{Sn}(\gamma, n)$ was studied with the view of the production of ^{117m}Sn for biomedical researches.

Radioanalytical Investigations

RFA, γ - and neutron-activation analyses of soil, moss and ecological samples from Bulgaria, Romania and Russia with the use of nuclear-physical methods of the analysis were carried out.

State of Radioactive Elements in Aqueous Medium

1. The distribution of U(VI), Ce(III) and Nd(III) in the system soil-solution was investigated (Bulgaria).
2. The distribution ^{237}U in the system humus acid-solution was investigated (England, Manchester's University).

The main results were published in [35–44].

REFERENCES

1. Oganessian Yu. Ts. et al. // Proc. of the Intern. Symp. on Physics of Unstable Nuclei «ISPUN07», Hoi An, Vietnam, July 3–7, 2007 / Ed. by Dao Tien Khoa et al. Singapore, 2008. P. 353–361.
2. Stefanini A. M. et al. // Phys. Rev. C. 2008. V. 78. P. 044607-1–044607-5.
3. Hauschild K. et al. // Ibid. V. 77. P. 047305.
4. Hauschild K. et al. // Ibid. V. 78. P. 021302(R).

5. Yeremin A. et al. // Nucl. Instr. Meth. B. 2008. V. 266. P. 4137–4142.
6. Kozulin E. M. et al. // Pribory i Tekhnika Eksperimenta. 2008. No. 1. P. 51–66.
7. Knyazheva G. N. et al. // Part. Nucl. Lett. 2008. V. 5, No. 1(143). P. 40–52.
8. Prokhorova E. V. et al. // Nucl. Phys. A. 2008. V. 802. P. 45–66.
9. Itkis M. G., Knyazheva G. N., Kozulin E. M. // Proc. of the First Workshop on State of the Art in Nuclear Cluster Physics «SOTANCP2008», Strasbourg, France, May 13–16, 2008; Intern. J. Mod. Phys. E. 2008. V. 17, No. 10. P. 2208.
10. Kamanin D. V. et al. // Ibid. P. 2250–2254.
11. Pyatkov Yu. // Ibid. P. 2226–2230.
12. Golovkov M. S. et al. The ^8He and ^{10}He Spectra Studied in the (t, p) Reaction // Phys. Lett. B (submitted); Archiv PLB 2008arXiv0804.0310G.
13. Fomichev A. S. et al. Properties of Very n -Rich He Isotopes // Eur. Phys. J. A (submitted).
14. Chudoba V. et al. Quest for the ^{10}He Nucleus // Proc. of the Intern. Conf. ASI-Prague-2007; Eur. Phys. J. A. Special Topics. 2008 (in press).
15. Grigorenko L. V. et al. Soft Dipole Mode in ^8He // Part. Nucl. Lett. (in press).
16. Krupko S. A. et al. Complete and Incomplete Fusion of ^6He and ^6Li Projectiles with Medium Mass Targets at Energy $\sim 10\text{A MeV}$ // Book of Abstr. «FUSION'08», Chicago, USA, Sept. 21–26, 2008. P. 50 (to be published in «World Scientific»).
17. Penionzhkevich Yu. E. et al. Complete and Incomplete Fusion of ^6Li Ions with Bi and Pt // J. Phys. G: Nucl. Part. Phys. (in press).
18. Lukyanov S. M. et al. Study of the $2n$ -Evaporation Channel in the $^4,6\text{He} + ^{206,208}\text{Pb}$ Reactions // Phys. Lett. B. (submitted).
19. Skobelev N. K. et al. // Part. Nucl. Lett. (in press).
20. Penionzhkevich Yu. E. Physics with Beams of Radioactive Nuclei // Phys. At. Nucl. 2008. V. 71. P. 1127; Yad. Fiz. 2008. V. 71. P. 1155.
21. Zagrebaev V., Greiner W. // Phys. Rev. C. 2008. V. 78. P. 034610.
22. Zagrebaev V., Greiner W. // Phys. Rev. Lett. 2008. V. 101. P. 122701.
23. Zagrebaev V., Greiner W. // J. Phys. G: Nucl. Part. Phys. 2008. V. 35. P. 125103.
24. Zagrebaev V. I. // Phys. Rev. C. 2008. V. 78. P. 047602.
25. Zagrebaev V. I., Samarin V. V. // Izv. RAN (Bull. of the Rus. Acad. of Sciences: Physics). 2008. V. 72, No. 3. P. 274–277.
26. Denikin A. S. et al. // J. Phys. G. (in press); nucl-th/0801.4550.
27. Ryabov E. G. et al. // Phys. Rev. C. 2008. V. 78. P. 044614.
28. Zagrebaev V. I. et al. <http://nrv.jinr.ru/nrv>
29. Aritomo Y., Hanappe F. // Nucl. Phys. A. 2008. V. 805. P. 534–536.
30. Antonova I. V. et al. // Solid State Phenomena. 2008. V. 131–133. P. 541–546.
31. Burlacu A. et al. // Nanotechnology. 2008. V. 19. P. 215714–215721.
32. Gordo P. M. et al. // Appl. Surface Sci. 2008. V. 255, Iss. 1. P. 254–256.

33. *Nazarov M. M. et al. // Rad. Measurements. 2008. V. 43, Suppl. 1. P. S591–S593.*
34. *Gikal B. N. et al. // Part. Nucl. Lett. 2008. V. 5, No. 1(143). P. 59–85.*
35. *Molokanova L. G. et al. // J. Appl. Chem. 2008. V. 81, No. 3. P. 480–485.*
36. *Balykin V. I. et al. // Izv. RAN (Bull. of the Rus. Acad. of Sciences: Physics). 2008. V. 72, No. 2. P. 224–228.*
37. *Ramirez P. et al. // Nanotechnology. 2008. V. 19. P. 315707.*
38. *Gillespie D. et al. // Biophys. J. 2008. V. 95. P. 609–619.*
39. *Apel P. Yu. et al. // Rad. Measurements. 2008. V. 43, Suppl. 1. P. 552–559.*
40. *Schulz A. et al. // Ibid. P. 612–616.*
41. *Kravets L. I. et al. // Nanotechnology. 2008. No. 1. P. 48–51.*
42. *Kravets L. I. et al. // Ibid. P. 43–48.*
43. *Didyk A. Yu. et al. // Perspective Materials. 2008. No. 4. P. 45–51.*
44. *Amirhanov I. V. et al. // J. Surface Investigation. X-ray, Synchrotron and Neutron Techniques. 2008. V. 2, No. 3. P. 331–339.*